Large piezoresistivity phenomenon in SiCN – (La , Sr) MnO 3 composites

Makarand Karmarkar, Gurpreet Singh, Sandeep Shah, Roop L. Mahajan, and Shashank Priya

Citation: Applied Physics Letters **94**, 072902 (2009); doi: 10.1063/1.3078271
View online: http://dx.doi.org/10.1063/1.3078271
View Table of Contents: http://scitation.aip.org/content/aip/journal/apl/94/7?ver=pdfcov
Published by the AIP Publishing

Large piezoresistivity phenomenon in SiCN–$(La,Sr)MnO_3$ composites

Makarand Karmarkar,[1] Gurpreet Singh,[2] Sandeep Shah,[3] Roop L. Mahajan,[2,4] and Shashank Priya[1,4,a)]

[1]*Center for Energy Harvesting Materials and Systems (CEHMS), Virginia Polytechnic Institute and State University, Blacksburg, Virginia 24061, USA*
[2]*Institute for Critical Technology and Applied Science (ICTAS), Virginia Polytechnic Institute and State University, Blacksburg, Virginia 24061, USA*
[3]*Center for Aircraft Structural Life Extension, HQ USAFA/DFEM, United States Air Force Academy, Colorado 80840, USA*
[4]*Department of Engineering Science and Mechanics, Department of Mechanical Engineering, Virginia Polytechnic Institute and State University, Blacksburg, Virginia 24061, USA*

(Received 19 October 2008; accepted 12 January 2009; published online 17 February 2009)

We present the results on SiCN–$(La,Sr)MnO_3$ (LSMO) composites correlating the observed large piezoresistance behavior with the microstructural features and defect chemistry. Scanning electron microscopy characterization revealed the presence of self-assembled periodic microvalleys in the microstructure with width of 1–5 μm and depth of 600–1000 nm. The microvalleys act as stress concentration points providing change in volume with applied stress. High resolution transmission electron microscopy measurements conducted on composites showed that LSMO grains consist of SiCN phase but no inclusions were observed. © *2009 American Institute of Physics*.
[DOI: 10.1063/1.3078271]

In recent decade, $(La_xSr_{1-x})MnO_3$ (LSMO) ceramics have been investigated widely due to the existence of colossal magnetoresistance.[1,2] Recently, we have reported large magnitude of piezoresistance coefficient in Nb_2O_5 modified $La_{0.8}Sr_{0.2}MnO_3$ (LSMO) polycrystalline ceramics.[3–5]

Polymer derived ceramics offer the high temperature materials that are otherwise difficult to be synthesized and open new possibilities for developing smart composites. Several nonoxide ceramics have been synthesized starting from molecular precursor in the systems Si–B–C–N, Si–B–C–N–O and Si–C–N.[6] Recent investigation on SiCN ceramic derived by thermal decomposition of a liquid-phase polyurea(methyvinyl) silazane shows promising piezoresistance behavior.[7] In addition, SiCN shows excellent high temperature creep and oxidation resistance.[8] Thus, the composite of this material with LSMO could provide more multifunctional properties of piezoresistivity, magnetization, and mechanical strength.

LSMO was synthesized by initial mixing of oxide and carbonate powders corresponding to 5 mol % Nb-modified LSMO ($x=0.2$), followed by calcination in alumina crucible at 1000 °C for 4 h. Calcined powders were crushed and ball milled for 24 h using 10 mm diameter grinding media in ethanol. While SiCN powder was synthesized by cross linking, followed by pyrolysis of liquid-phase polyurea (methyvinyl) silazane (Ceraset™, Kion Specialty Polymers, Charlotte, NC) at 375 and 1100 °C, respectively, under continuous nitrogen flow. The composites were prepared by mixing LSMO with SiCN in mortar pestle for 1 h followed by sintering at 1300 °C for 3 h in air. The volume percent of SiCN in LSMO was fixed at 3%, 6.5%, and 12.35%. The samples for piezoresistivity measurements were prepared by machining square pieces of dimensions $(5.0\times5.0\times1.5)$ mm^3 and painting a high temperature silver electrode Dupont® 6160 on (5×1.5) mm^2 area. The painted electrodes were then fired at 650 °C for 1 h to obtain a good electrical contact. Resistivity measurements as a function of applied force were done on the square samples by compressing them between two highly polished flat surfaces using Instron™ mechanical tester. A compressive load of up to 200 N was applied uniaxially at the rate of 20 N/min onto the sample. The resistance change in the samples was recorded by an Agilent® $6\frac{1}{2}$ digit multimeter. For each measurement approximate load intervals of 20 N were chosen, and the load was held constant at each step for 3 min allowing the resistance values to be stabilized. After the 3 min holding time the compressive loading was resumed at the same rate.

Figure 1(a) shows the resistivity of the sintered samples. A continuous increase in the resistivity was observed with increasing volume fraction of SiCN in LSMO. There is large jump in the magnitude of resistivity at 4 vol % SiCN. The data in this figure were fitted using the Sigmoidal–Boltzmann equation given as

$$R = \frac{R_1 - R_2}{1 + \exp\left(\frac{V - V_o}{dV}\right)} + R_2,$$

where R_1 $(=43.82\times10^{-4}\ \Omega\ \text{m})$ and R_2 $(=6.82\times10^{-4}\ \Omega\ \text{m})$ represent the final and initial magnitude of the resistivity, V is the volume fraction of SiCN, V_o (=5.24 vol %) represents the volume fraction for 50% change in resistivity, and dV represents the steepness of the change (=−0.834). Clearly, the saturation in the magnitude of resistivity occurs at 12.35 vol % SiCN indicative of the percolation threshold. Figure 1(b) shows the change in resistivity with increasing compressive force. The resistivity change for 3 and 6.5 vol % SiCN was quite small exhibiting a peak at specific magnitude of force. The position of the peak increases with increasing volume fraction of SiCN. The samples with 12.35 vol % SiCN showed large change in resistivity of the order of 4% at an applied force of 2 MPa. This is a significant enhancement in the magnitude of piezoresistive coeffi-

a)Author to whom correspondence should be addressed. Electronic mail: spriya@vt.edu.

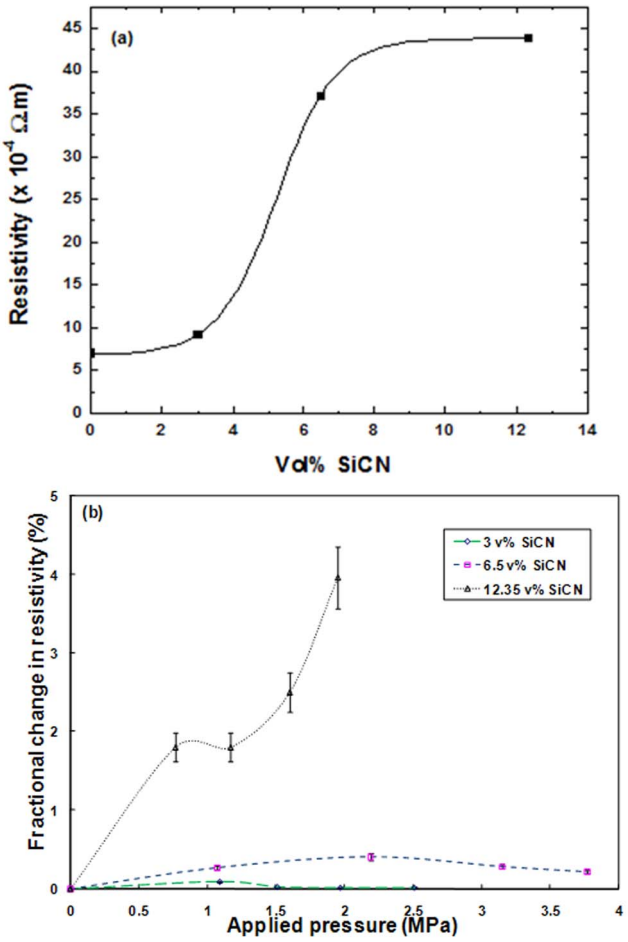

FIG. 1. (Color online) (a) Change in resistivity of LSMO-SiCN composite with varying volume fraction of SiCN and (b) change in resistance with applied force for composites with three different volume fractions of SiCN.

cient compared to pure and Nb-modified LSMO. It is expected that this composition will also exhibit peak behavior at the higher stress level, however, our measurements were limited due to the stability of output value. At higher volume fraction of SiCN the samples exhibited a microvalley-type microstructure, which could be the reason for prolonged time constant.

SEM-energy dispersive spectroscopy was performed using the field emission SEM. The surface microstructure of 12.35 vol % SiCN sample showed large porelike regions as shown in Fig. 2(a), which we refer to as microvalleys. The reason for the existence of these valleys is explained as following. The sample did not show any microcracks so it is assumed here that the strain generated during sintering due to differing thermal shrinkages is absorbed in the ceramics. The density of ceramics decreased with increasing volume percent of SiCN, which may be related to the composite structure formation and incorporation of SiCN in the microstructure. The thermal shrinkage for LSMO has been reported to be in the range of 12% to 14% in the sintering range of 1300 °C.[9] The thermal shrinkage for SiCN during cross linking and pyrolysis is about 30%.[10] Recent results have shown that SiCN undergoes microstructural changes until 1400 °C, still remaining amorphous with less than 5% crystallinity.[11] The structure of this amorphous phase at 1280 °C consists of sintering related open and closed pores distributed at nanoscale and an additional molecular structure related pore that

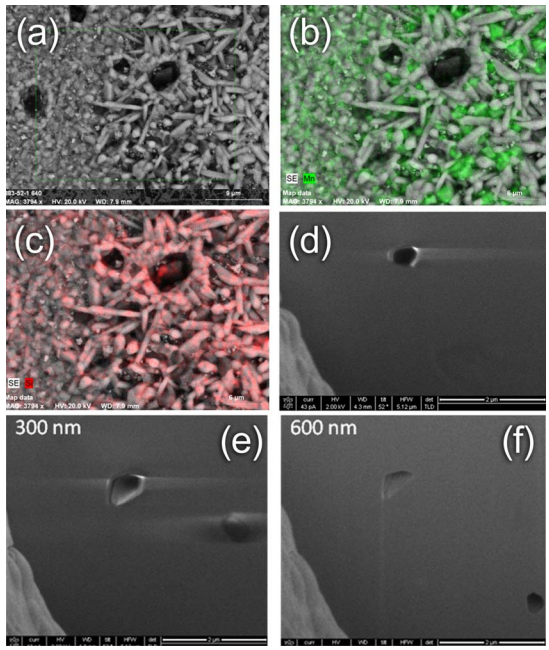

FIG. 2. (Color online) (a) Surface microstructure of LSMO—12.35 vol % SiCN, [(b) and (c)] elemental analysis for Si and Mn, and [(d)—(f)] depth profiling of the microvalleys.

can be correlated with electrical characteristics. We associate the formation of microvalleys in Fig. 2(a) primarily to compensate the strain developed during the sintering and secondarily to the growth of inherent porosity present in the SiCN ceramic after sintering at 1300 °C. Figures 2(b) and 2(c) show the distribution of Si and Mn elements in the sintered microstructure in the vicinity of microvalleys. The element Si is mainly present in the leafletlike structure, which is amorphous SiCN. This indicates that SiCN partitions within the matrix LSMO and is present as a second phase with leafletlike geometry in the vicinity of microvalleys. Figures 2(d)–2(f) are the collection of the cross-sectional images of the microvalleys (depth profiling) performed by using the focused ion beam SEM (FIB, FEI-Helios Nanolab 600). The height of the valley was found to be in the range of 600–1000 nm and their width in the range of 1–5 μm. Thus, for a 1.5 mm thick sample the microvalley distribution can be assumed to be a disconnected network. Using SEM analysis, the density of microvalleys was estimated to be in the range of 600–1000 mm^{-2}. The distribution of microvalleys appear to be random, however, their size is affected by the presence of other microvalleys in its vicinity. If the microvalleys were close to each other the growth was inhibited while those far apart from each other had size in the range as described in Fig. 2. This size distribution of microvalleys is believed to be significant factor in providing peak behavior as shown in Fig. 1(b). A Gaussian fit to the data in Fig. 1(b) indicates that composite with 12.35 vol % SiCN will provide ~7.5% fractional change in resistivity at the stress magnitude of ~4.5 MPa.

The microstructure shown for LSMO-SiCN composites in Fig. 2 can be used to explain the results in Fig. 1. Recent study by Das *et al.*[12] on $(La_{0.67}Ca_{0.33})MnO_3$–SiCN composite sintered at 1100 °C for 2 h showed that resistivity changes significantly with addition of 5–10 vol % of SiCN. The results were explained on the basis of growth of particle size of LCMO (SiCN acting as sintering additive) and small

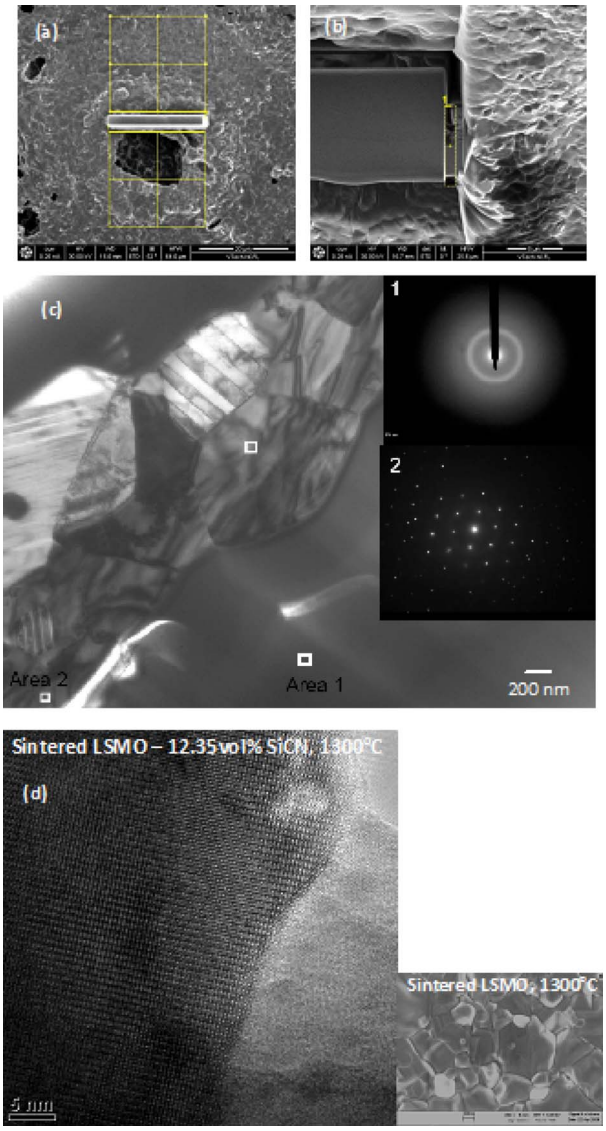

FIG. 3. (Color online) (a) Deposition of the platinum close to microvalley interface for machining the sample (at 52° tilt), (b) machining area showing the sample was released at the interface, (c) TEM microstructure near the SiCN/LSMO interface, and (d) HRTEM image of the LSMO grains far from the microvalley (subset: pure LSMO ceramic sintered at 1300 °C).

polaron hopping transport (presence of Mn^{+3} state). Zhang *et al.*[7] studied the piezoresistive behavior of pure SiCN ceramics sintered at 1400 °C for 4 h. A large gauge factor of 1000–4000 was measured in their experiments. The results were explained on the basis of tunneling percolation mechanism, which operates due to the presence of conducting graphene sheets in the microstructure formed from the free carbon. The applied stress causes change in the distance between graphene sheets leading to change in the resistivity. Combining the results of these two prior studies it can be hypothesized that piezoresistive behavior in LSMO-SiCN composites will be influenced by the presence of mixed Mn valence state, large grain size of LSMO, and nanodomain structure due to the formation of conducting graphene sheets based structure. Our TEM analysis of interface structure [close to the leaflet in Fig. 2(a)] has shown the formation of twin-bandlike regions in LSMO grains as shown in Figs. 3(a)–3(c). The size of these bands was dependent on the distance from the SiCN/LSMO interface. The formation of these bands gives us preliminary indication toward the presence of nanodomains. It is interesting to note that the grains farther from the SiCN microvalley had the presence of regular bands, while those closer to it had small size and scattered distribution. Further TEM investigation was conducted on LSMO grains farther from the microvalley to seek the presence of SiCN nanodomains. The presence of SiCN nanodomains throughout the matrix will explain the large response.

HRTEM imaging was conducted by using the FEI Titan 300 microscope operated in a Scanning and conventional TEM mode at 200 kV. Figure 3(d) shows the HRTEM structure of LSMO grains in the composite far from the microvalleys using conventional TEM mode. We did not find the presence of any secondary structure in the grains or any inclusions on the boundaries. However, elemental analysis revealed the presence of elements Si, C, and N in the grains (please refer to the supplemental information performed using TEM mode).[13] This gives us indication that there is existence of nanodomains in the structure but it would require more analysis using techniques such as small angle x-ray scattering to reveal their distribution. The high density and sharp grain boundary of LSMO grains in Fig. 3(d) also indicates that sintered ceramic had low concentration of defects. The subset of this figure shows the pure LSMO ceramic sintered at 1300 °C. Comparing with composite microstructures there was only slight increase in the grain size. Thus, we associate the observed piezoresistive behavior with presence of mixed valence state, which results in changes in Mn–O bond length, presence of nanodomains, and alternation in total volume of the material due to the stress concentration in the microvalleys. TEM results indicate distribution of SiCN nanodomains over the whole microstructure.

G. Singh would like to thank D. Ahn at the University of Colorado for useful discussions on SiCN composites. Thanks are also due to instrument specialists at the Nano Characterization and Fabrication Laboratory (NCFL) and ESM. The authors (M.K. and S.P.) would like to acknowledge financial support from the Office of Naval Research (Grant No. N00014-08-1-0654)

[1] C. N. R. Rao, R. Mahesh, A. K. Raychaudhuri, and R. Mahendiran, J. Phys. Chem. Solids **59**, 487 (1998).
[2] P. G. de Gennes, Phys. Rev. **118**, 141 (1960).
[3] V. Sharma, M. R. Hossu, W. H. Lee, A. R. Koymen, and S. Priya, Appl. Phys. Lett. **89**, 202902 (2006).
[4] V. Sharma, M. Hossu, W. H. Lee, A. R. Koymen, and S. Priya, J. Mater. Sci. **42**, 9841 (2007).
[5] V. Sharma, M.S. thesis, UT Arlington, 2006.
[6] R. Riedel, G. Mera, R. Hauser, and A. Klonczynski, J. Ceram. Soc. Jpn. **114**, 425 (2006).
[7] L. Zhang, Y. Wang, Y. Wei, W. Xu, D. Fang, L. Zhai, K.-C. Lin, and L. An, J. Am. Ceram. Soc. **91**, 1346 (2008).
[8] R. Riedel, L. M. Ruwisch, L. An, and R. Raj, J. Am. Ceram. Soc. **81**, 3341 (1998).
[9] D. Grossin and J. G. Noudem, Solid State Sci. **6**, 939 (2004).
[10] Y. Liu, L.-A. Liew, R. Luo, L. An, M. L. Dunn, V. M. Bright, J. W. Daily, and R. Raj, Sens. Actuators, A **95**, 143 (2002).
[11] H. Störmer, H.-J. Kleebe, and G. Ziegler, J. Non-Cryst. Solids **353**, 2867 (2007).
[12] D. Das, A. Saha, C. M. Srivastava, R. Raj, S. E. Russek, and D. Bahadur, J. Appl. Phys. **95**, 7106 (2004).
[13] See EPAPS Document No. E-APPLAB-94-100905apl for x-ray energy dispersive spectroscopy data corresponding to Fig. 3(d), taken from TEM operating at 200 kV in the conventional mode. Energy peaks corresponding to Si, C. N. and O are visible. For more information on EPAPS, see http://www.aip.org/pubservs/epaps.html.